



red earth
engineering

Dr Marcelo Llano

Breaching the gap between geotechnical and hydraulic engineering to improve tailings dam breach studies through large deformation modelling

27 October 2020



Outline

Motivation

Flowability of tailings (Mobility)

Material Point Method (MPM) – large deformation modelling

The effective stress concept, strength and rheology

Case Studies

Summary and final thoughts

Motivation

CDA (2021) Technical Bulletin: Tailings Dam Breach Analysis

5.2 Tailings characterisation: “Flow liquefaction results in **large deformations** and directly impacts the volume of tailings that can be released during a breach”.

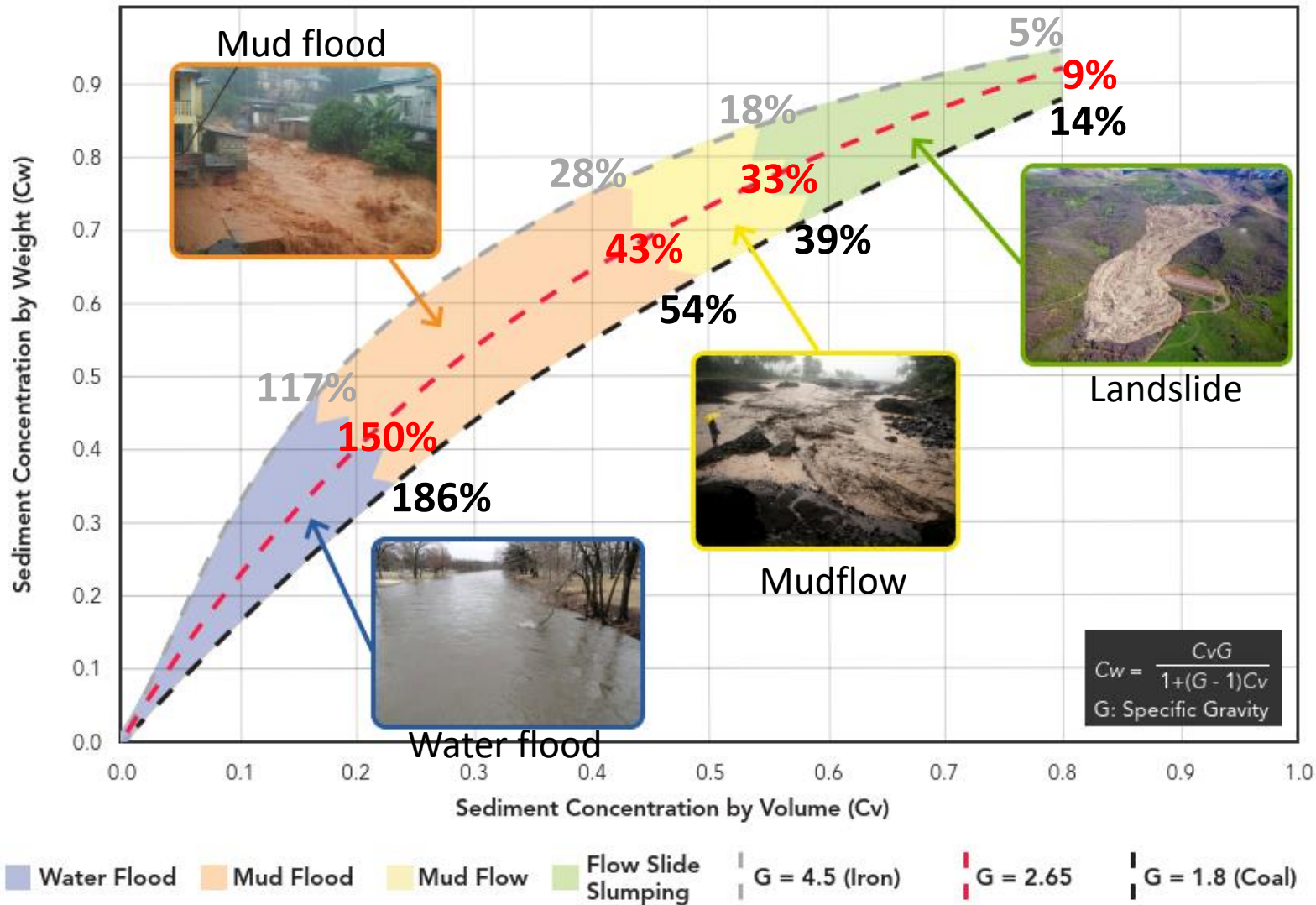
5.3 Rheological behaviour: “The measurement of yield stress and viscosity are often conducted for tailings with a volumetric **solid concentration less than 45-55%**. Yield strength and viscosity increase exponentially and become very sensitive to the solids concentration when the solids concentration is close to a threshold, illustrating the influence of water content on the rheological behaviour”....

Liquid limit, traditionally ranges between 1.7kPa to 2.3kPa. Soils at the plastic limit have around 100 times the undrained shear strength measured at the liquid limit.

“Although the concepts of viscosity and yield stress are commonly used in conventional fluid mechanics to characterise the shear properties of a fluid, they can be inadequate to describe some non-Newtonian flows with high solid concentrations in which the **particle-to-particle contacts become dominant** and control the flow”.

“... at higher solids concentrations the mechanisms of **compression and dilation may affect the tailings flows** and should be taken into account.”... “integration of the principles of advanced soil mechanics in combination with fluid mechanics and rheology can be used”.

Mobility of flow events (modified from CDA, 2021)

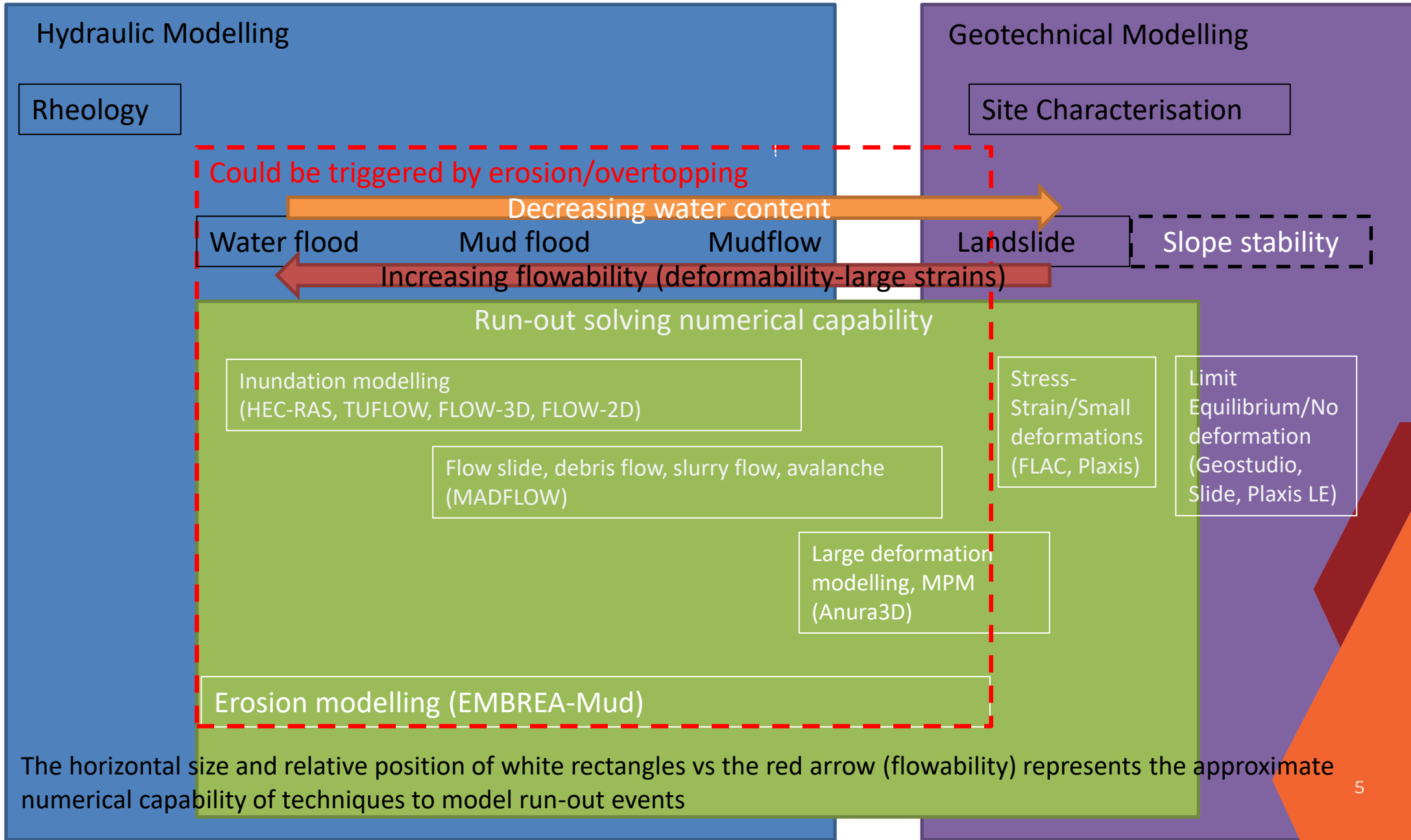


Percentages on the plot added by the author are equivalent gravimetric water content assuming 100% saturation. Note that lines in the plot for lower water contents might be different depending on the shrinkage limit.



Figure 8.1: Flow Types as a Function of Solids Concentration (Source: modified from Martin et al. 2019, adapted from Julien and O'Brien 1985)

Mobility of tailings in the context of modelling techniques



Material Point Method (MPM) Background - Marcelo

- 2012, MSc in Geotechnics – University of Brasilia, Brazil
Thesis: Material Point Method Applications to Geotechnical Engineering Problems
- 2016, PhD in Geotechnics – University of Brasilia, Brazil
(with an externship at the GEC in the University of Queensland)
Thesis: Experimental and Numerical Study of Geotechnical Engineering Problems Using the Material Point Method

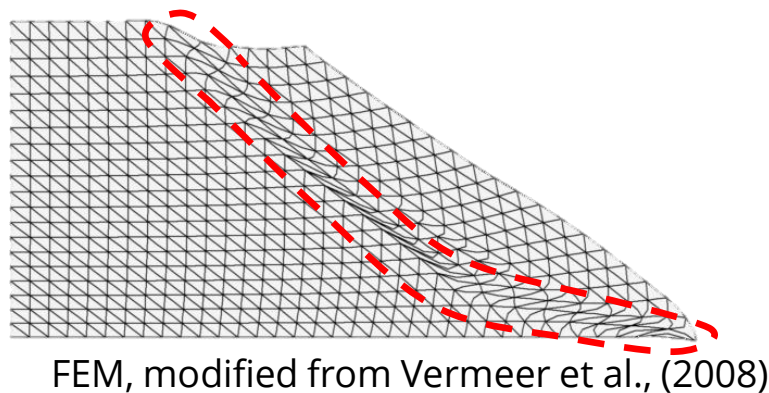
Around 30 scientific publications including two papers in *Géotechnique* and >100 citations

MPM Background - Introduction

BACKGROUND: Finite differences (used in FLAC) was introduced by Taylor in 1715. FEM- Finite Elements (used in Plaxis) was developed in the 1940s (Hrennikoff, 1941, Courant, 1942). Both tackle complex engineering problems for which there is no analytical solution based on continuum mechanics approach.

PROBLEM: The traditional formulations are not well suited to tackle large deformation problems.

ALTERNATIVE APPROACH: Meshfree or Meshless Methods (MPM) may solve the problem of simulating large deformations.



MPM, Llano-Serna (2012)

MPM Background - Relevance

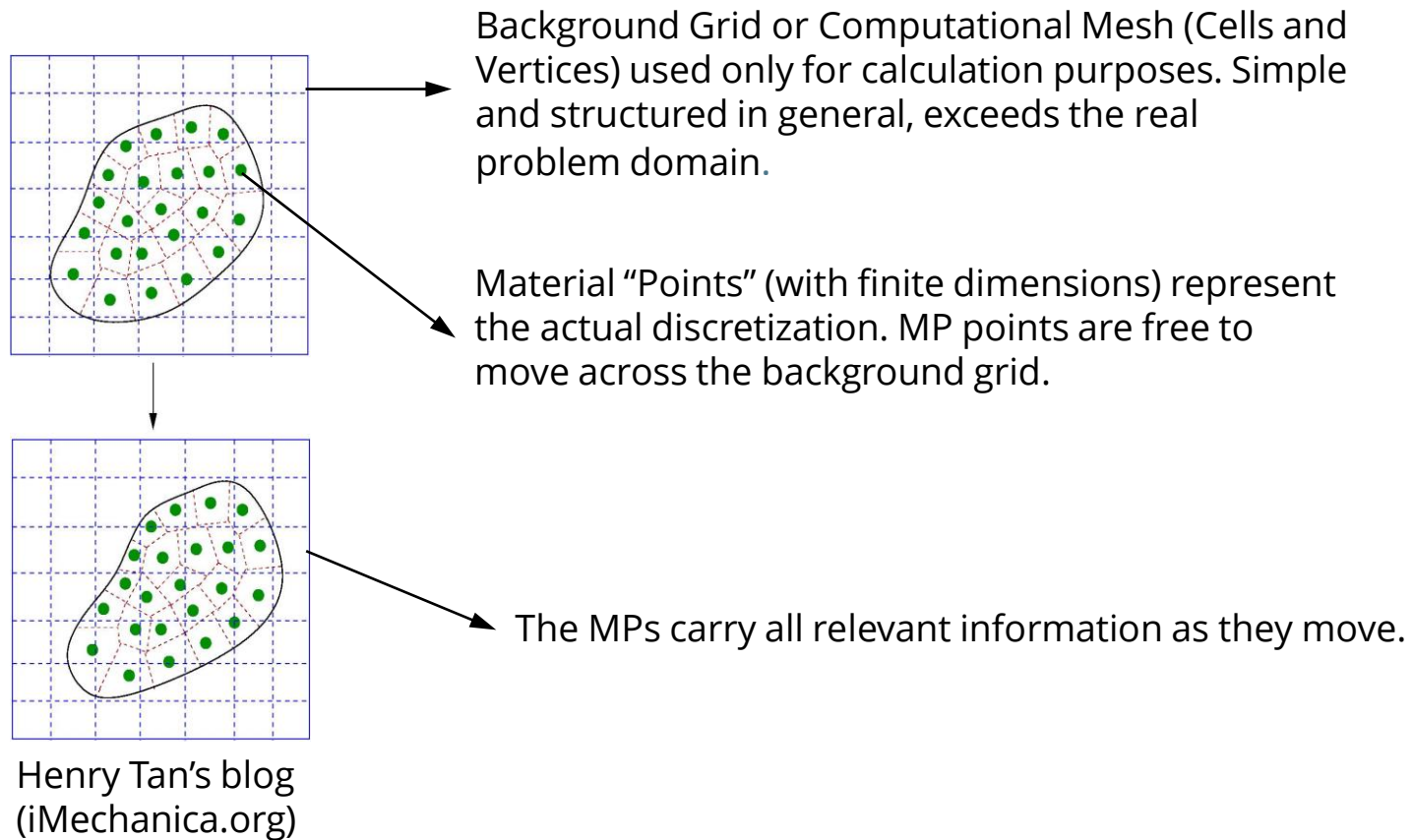
Large deformation phenomena are very common in Geotechnical Engineering

- STP, CPT, DMT, Fall cone test...
- Landslides, dam failure
- Piling

Classical numerical techniques fail to deal with large deformations



MPM Background – The idea

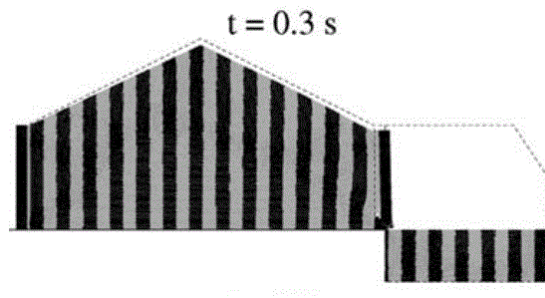


MPM development with emphasis on tailings dams- timeline

- 1964 - Particle in Cell (PIC) Method formulation (fluids) - Harlow
- 1994 – Material Point Method (PIC extension for solids) - Sulsky
- 1999 – First application in Geotechnical Engineering- Zhou et al. (Embankment settlement and geotextiles)
- 2010 – First application in slope stability and tailings dam failure (Aznalcollar) - Zabala
- 2017 – Rankine lecture on triggering and motion of landslides, Prof. Eduardo Alonso –UPC, Spain (Emphasis on MPM)
- 2017-2018 – Conceptual models of various run-out examples – The Author, while working at the GEC, UQ
- 2019 – MPM modelling of Brumadinho failure (Results included in the expert panel report) – The Author
- 2021 – MPM modelling of Cadia – Ian Pierce, Alba Yerro (Virginia Tech)
- 2021 - Contributions to the development of Tailings Dam

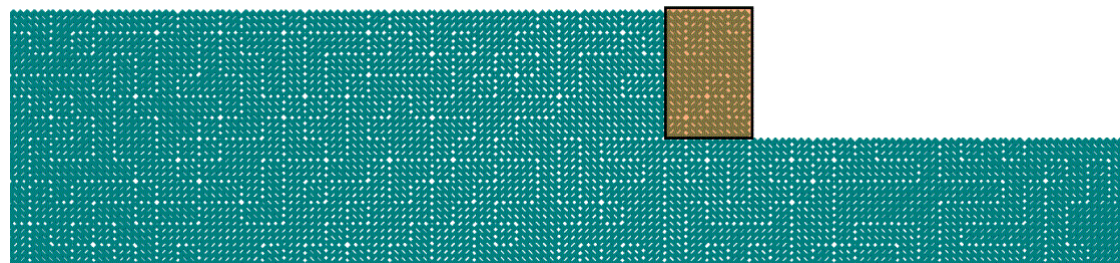
MPM examples – Geotechnical models, conceptual capabilities

Active/passive earth pressure



5.5m tall, 11.0m wide
Wieckowski (2004)

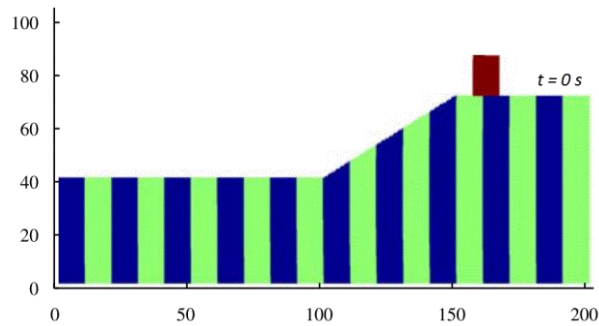
Wall movement : 0,0 cm



1.0m tall wall
Beuth et al. (2011)

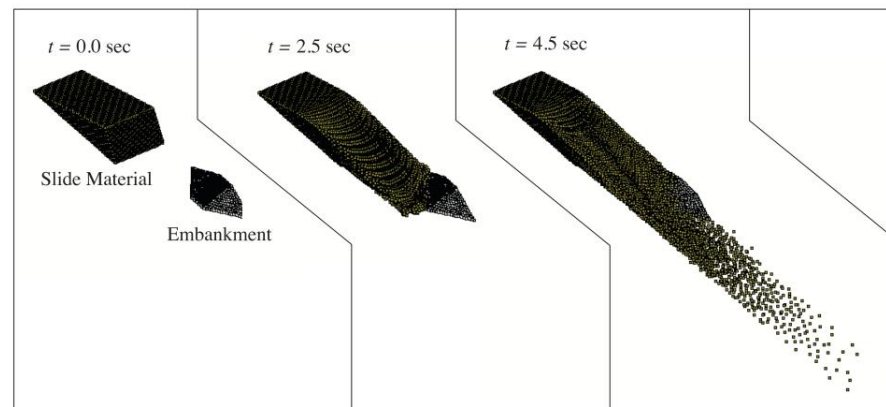
MPM examples – Geotechnical models, conceptual capabilities

Slope instability / erodible barriers



20.0m tall slope
Andersen (2010)

Shin et al. (2011)



Software available

Commercially available software do not exist to date. Several research packages exist.

Anura3D - <http://www.mpm-dredge.eu/> (Recommended)

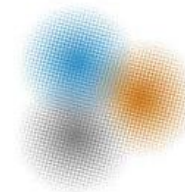
CB-Geo - <https://www.cb-geo.com/research/mpm/>

Uintah - <http://uintah.utah.edu/>

NairnMPM - <http://people.oregonstate.edu/~nairnj/>



UNIVERSITÀ
DEGLI STUDI
DI PADOVA



Anura3D

MPM Research Community

Modelling large deformation and soil–water–structure interaction

Partial summary 1

Large deformations in the context of geotechnical engineering

Large deformations are a common occurrence in the practice of geotechnical engineering. Unfortunately, tools to model and further understand some of the mechanisms when large deformation take place are limited (but exist).

In slope stability/dam engineering, engineers have trained and learnt to perform calculations to “avoid failure”, which in this field is understood as deformation (large or small) of a given slope. Despite significant progress in computational capacity, limit equilibrium techniques with no deformation involved are the most common approach.

Limit equilibrium will be challenged more often (but unlikely to disappear) as earthen structures grow due to commercial demand, international standards and guidelines are becoming more refined. An obvious step forward is a wider adoption of small deformation approaches for which the availability of commercial packages is vast.

The effective stress concept, strength and rheology

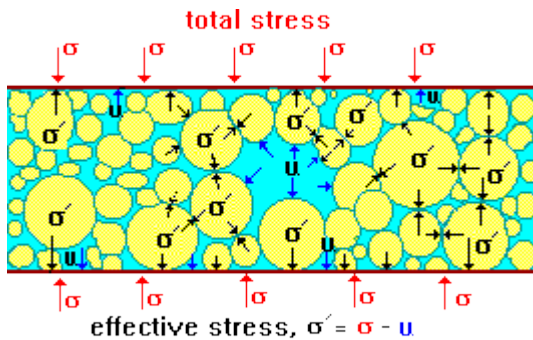
Meaning of effective stress (1925)

Trenchlesspedia.com

“Effective stress can be defined as the stress that keeps particles together. In soil, it is the combined effect of pore water pressure and total stress that keeps it together”.

Wikipedia.org

“Can be defined as the stress, depending on the applied tension and pore pressure, which controls the strain or strength behaviour of soil and rock (or a generic porous body)”.



Environment.uwe.ac.uk

$$\sigma'_v = \sigma_v - u$$

$$p' = \frac{\sigma'_1 + 2\sigma'_3}{3}$$

$$s' = \frac{\sigma'_1 + \sigma'_3}{2}$$

Most common (Easy but does not take horizontal stress into account)

Cambridge notation

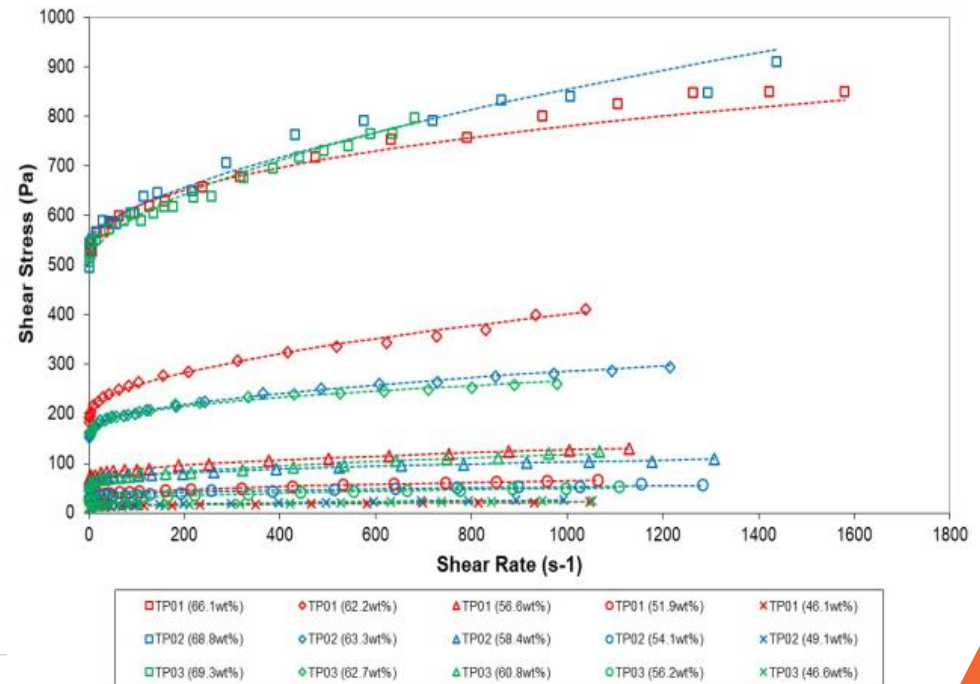
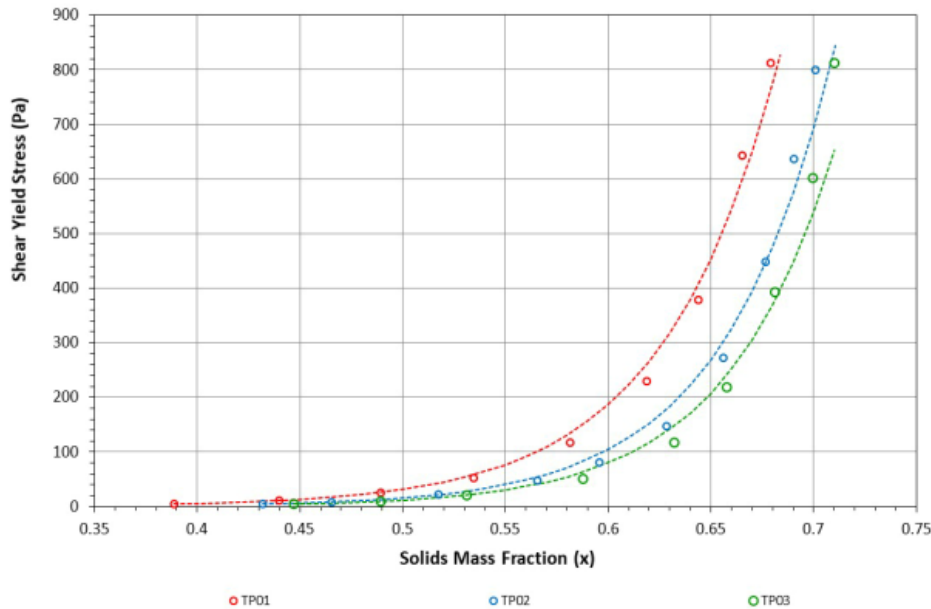
MIT notation, some authors use p' to refer to s' which makes it confusing

The effective stress concept, strength and rheology

Rheological characterisation

Conventionally includes shear yield stress vs solids mass fraction, and Shear stress vs shear rate.

Usually expressed in terms of total stresses. Is there an influence of effective stresses (i.e. different rheological behaviour varying with depth)?



The effective stress concept, strength and rheology

Soft Matter

RSC Publishing

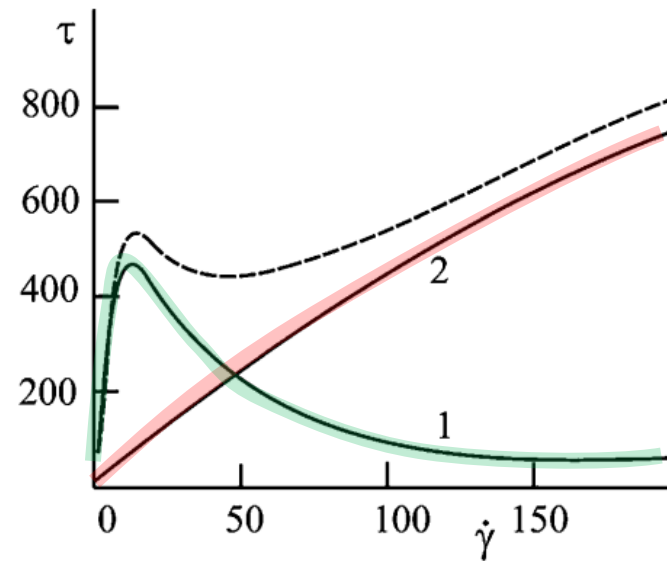
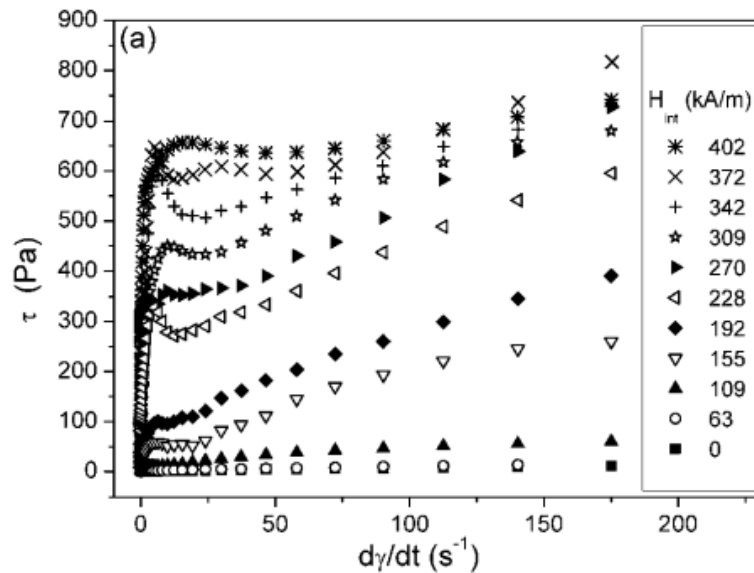
PAPER

[View Article Online](#)
[View Journal](#) | [View Issue](#)

N-Like rheograms of suspensions of magnetic nanofibers

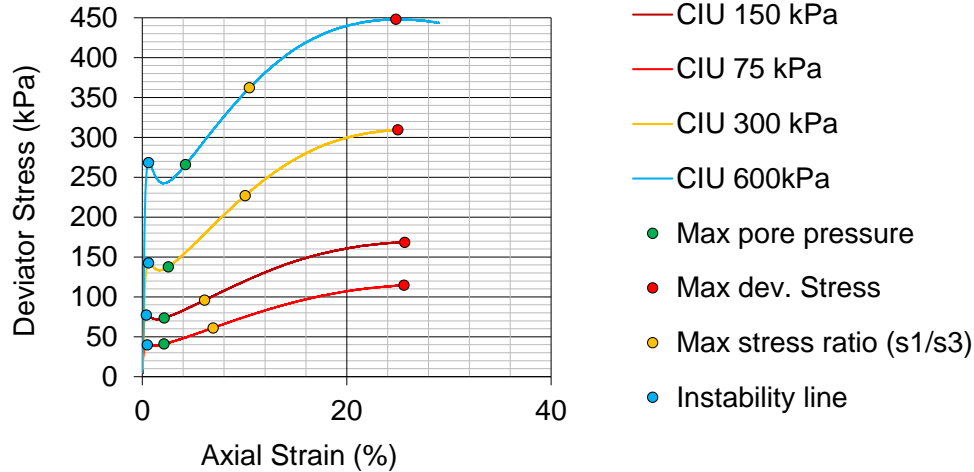
Cite this: *Soft Matter*, 2013, **9**, 1902

Andrey Zubarev,^{*a} Modesto T. López-López,^b Larisa Iskakova^a
and Fernando González-Caballero^b



“In the first type of aggregate, interfiber friction is not very strong and nanofibers could reorganise as the aggregate is tilted by the shear flow, given rise to a “paramagnetic” aggregate with changeable magnetisation. In the second type of aggregate, interfiber friction is so strong that nanofiber orientations are fixed and, thus, the magnitude and directions (along the aggregate main axis) of the magnetisation of the aggregates are fixed too.”

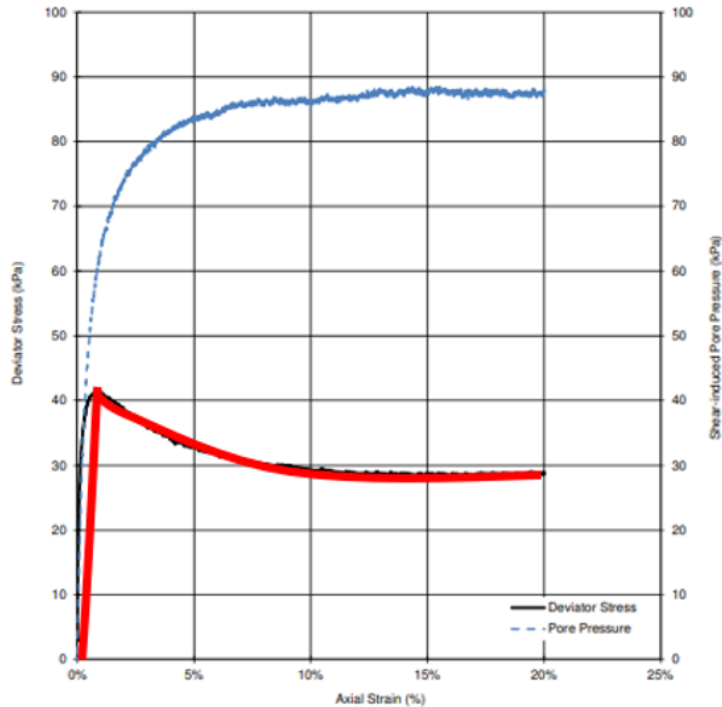
The effective stress concept, strength and rheology



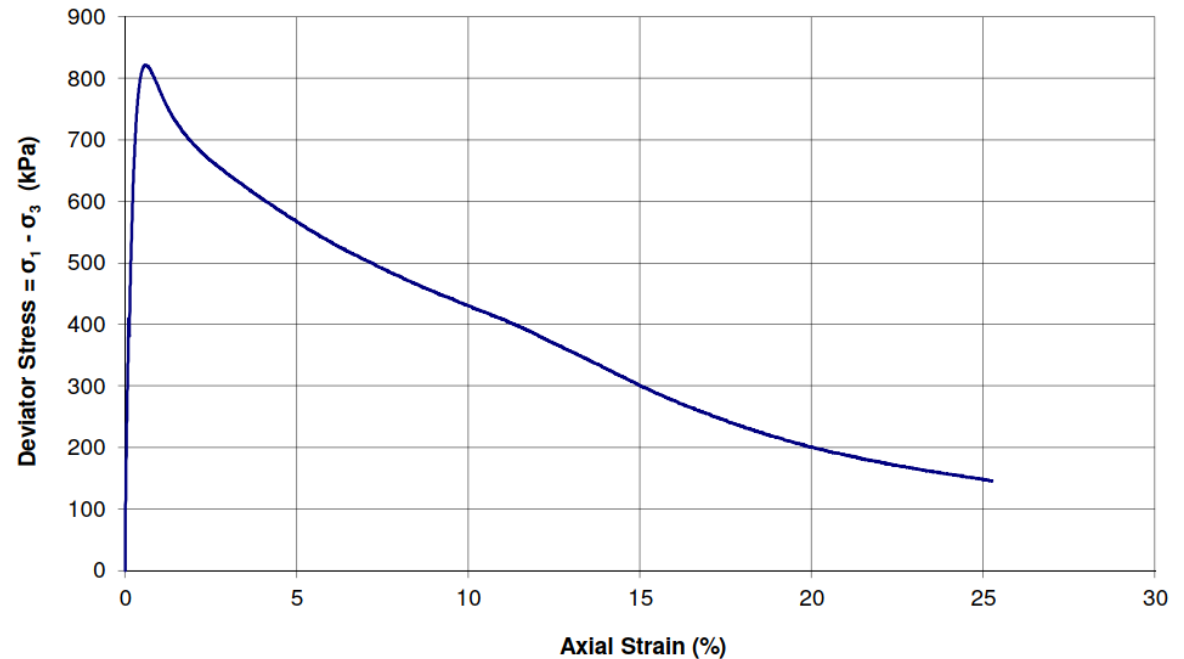
Tailings tested under conventional triaxial undrained compression for different effective stresses can also show N-like stress-strain curves. There is evidence of different responses with varying confinement stress.

One might have aggregate type one or two (In Zubarev's framework) dominating the response of tailings based on material characteristics. See Cadia and Brumadinho examples below.

CIU triaxial at 50kPa, from Appendix E, loose tailings properties. Cadia, Expert Review Panel.



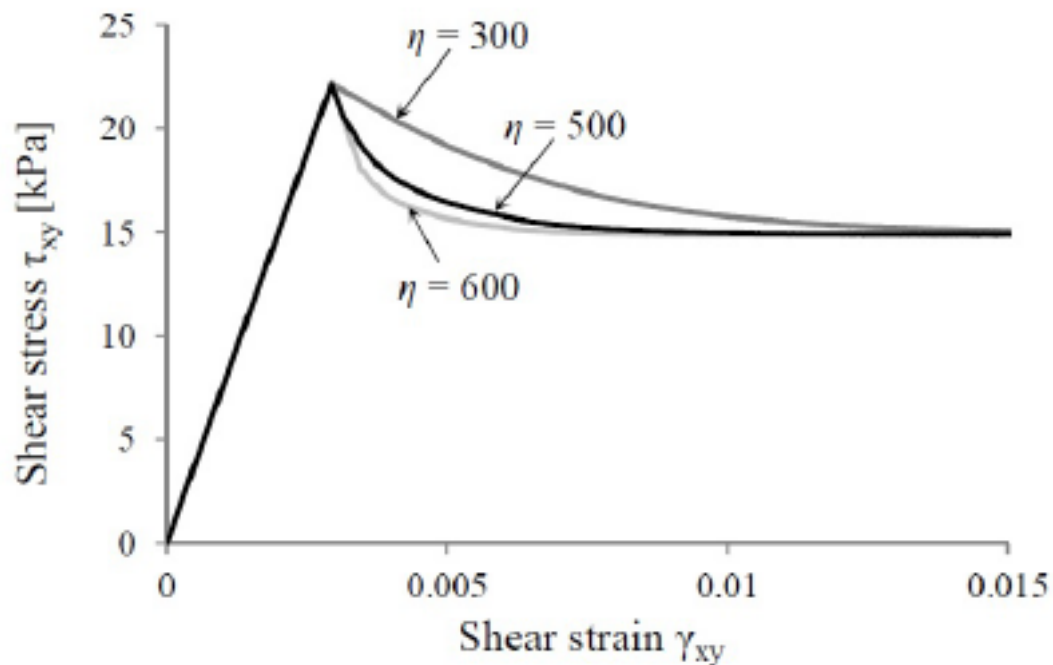
CIU triaxial at 2000kPa, test certificate from Appendix E, loose tailings properties. Feijao (Brumadinho), Expert Panel Report



The effective stress concept, strength and rheology

Model recommended to simulate strain softening

Brittleness may be simulated by introducing a strain-dependent parameters that controls the transition between peak frictional angle or peak cohesion to residual frictional angle or cohesion. The softening behaviour is accounted for by reducing the strength parameters with the accumulated plastic deviatoric strain.



Evolution of the shear stress with shear strain for several brittle responses

Partial summary 2

Constitutive behaviour of tailings during a breach event

The effective stress concept has been known to influence the mechanical response of granular arrangements during loading. Specifically, a MPM model can simulate the “initiation” of the failure and the transition between a static (solid) state through a deformation process that can result in liquefied tailings.

Limited rheological testing under confining stresses exist, available results suggest that confining pressures have an influence in the rheological response of materials, specially during the solid to fluid transition. See also Chen et al., (2008) and Jia et al., (2021).

A detailed study about the role of different constitutive models in MPM simulations of granular column collapses is presented by Fern and Soga (2016).

Case studies

Influence of deposit length and undrained shear strength on run-out distance (The Author, software:NairnMPM)

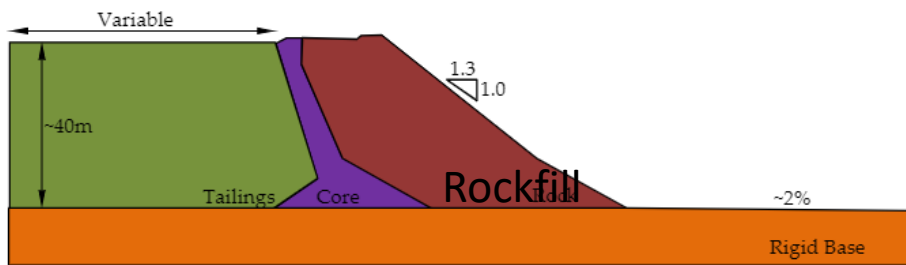


Figure 2 Cross-section analysed.

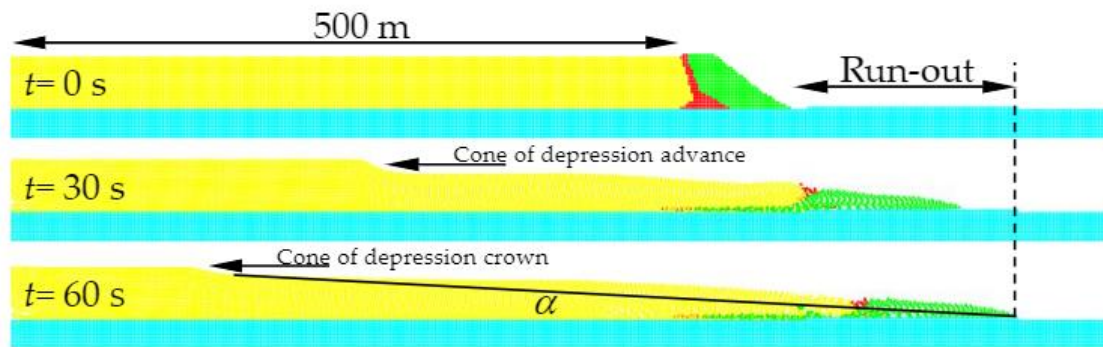
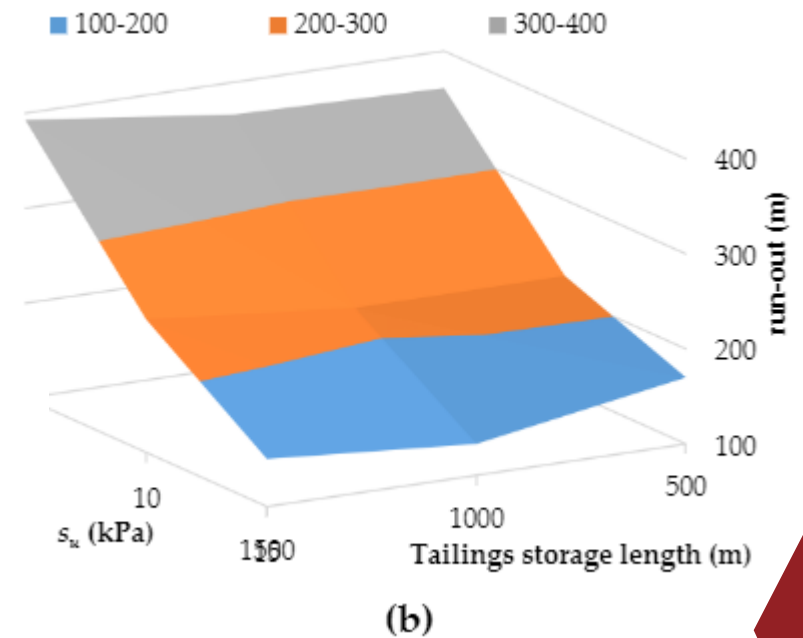


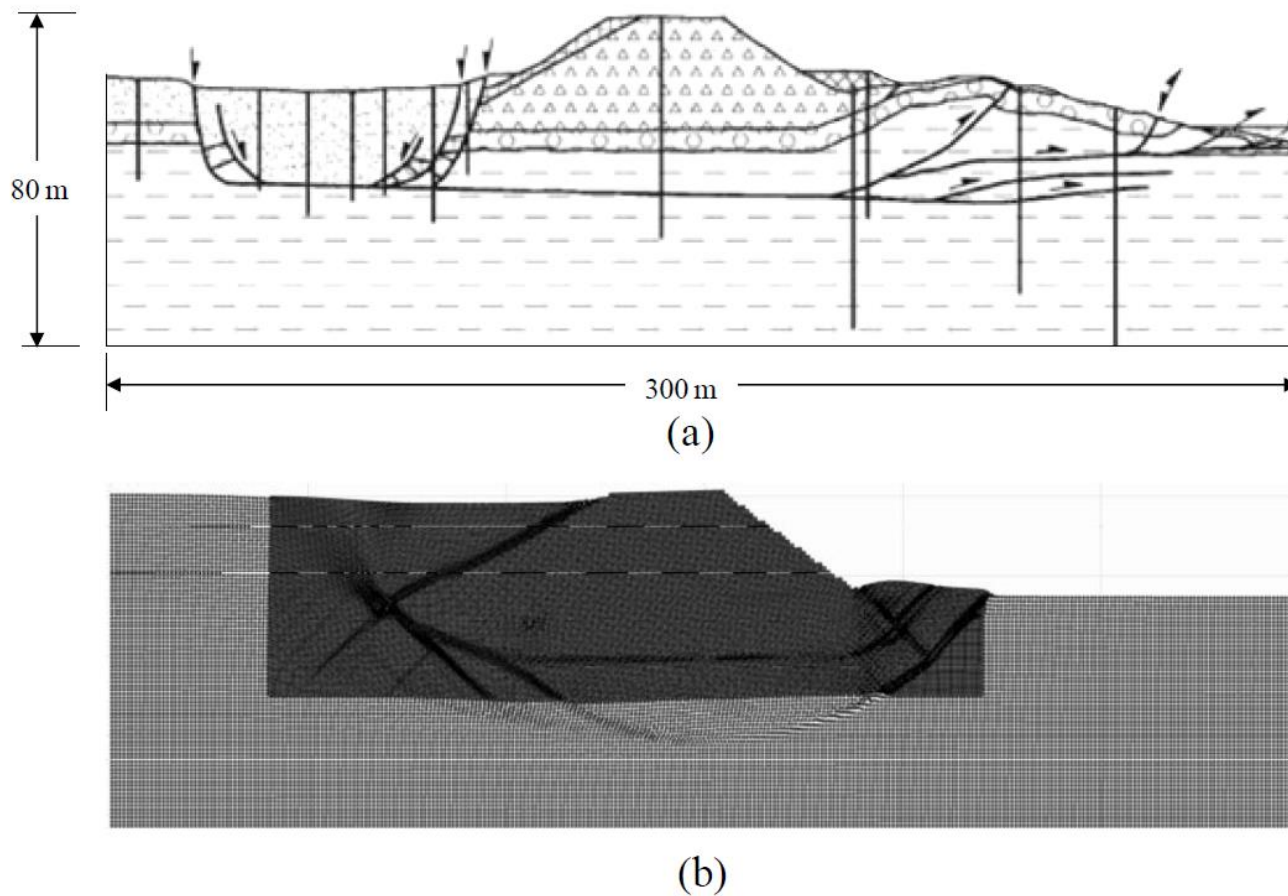
Figure 3 Time progression of run-out analysis resulting for a 500 m long storage containing tailings with $s_u = 15$ kPa.



(b)

Case studies

Aznalcollar (Los Frailes) – Zabala (2010)



Pore water pressures prevailing in the foundation clay at the time of the failure, with strength behaviour of brittle clay with low permeability was attributed as the main cause of the event.

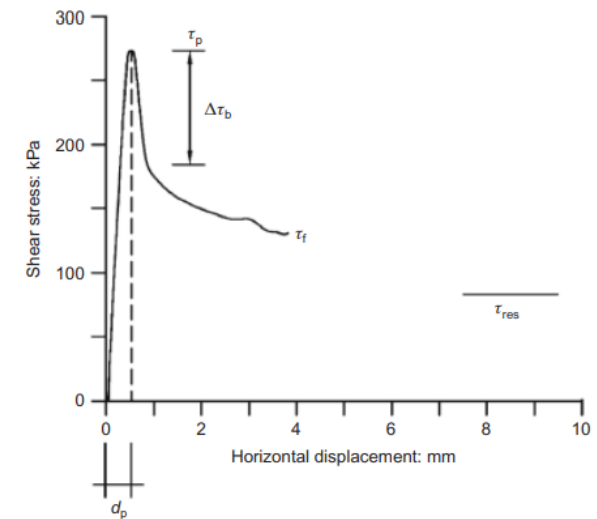


Fig. 4. Direct shear test on specimen of foundation clay; normal effective stress 400 kPa (Alonso & Gens, 2006a)

Case studies

Brumadinho – The Author (2019)

Using Anura3D

Table 4 summarises the MPM model results. The MPM model results were compared with the available video footage to assess the evolution of dam failure. At $t = 2$ seconds (s), a velocity of around 5 meters per second (m/s) was estimated within the body of the tailings behind the face. At $t = 5$ s, transverse cracks were observed on the video footage. The numerical model shows a concentration of deviatoric strain reaching unity at the toe of the dam that propagates upwards behind the berms at this stage. At $t = 7$ s, bulging of the face is evident from both the video recording and the model. Continued crest settlement and retrogression of multiple slip surfaces occurred in the model in a manner representative of the video footage. The kinematic plot in Figure 61. shows an approximate total acceleration of 3 m/s^2 from $t = 0$ s to $t = 10$ s when the failed mass reaches a maximum velocity of around 30 m/s (i.e., 100 km/hr). At $t = 15$ s the failure is well developed over the entire height of the dam; the run-out velocity shown in Figure 61 indicates values ranging between 25 m/s and 30 m/s.

In summary, this analysis showed that once the failure was initiated, it would develop into a series of retrogressive failure planes that would occur at a rate that matched the observations. This analysis provided further support for the strain-weakening relationship used in earlier analyses.

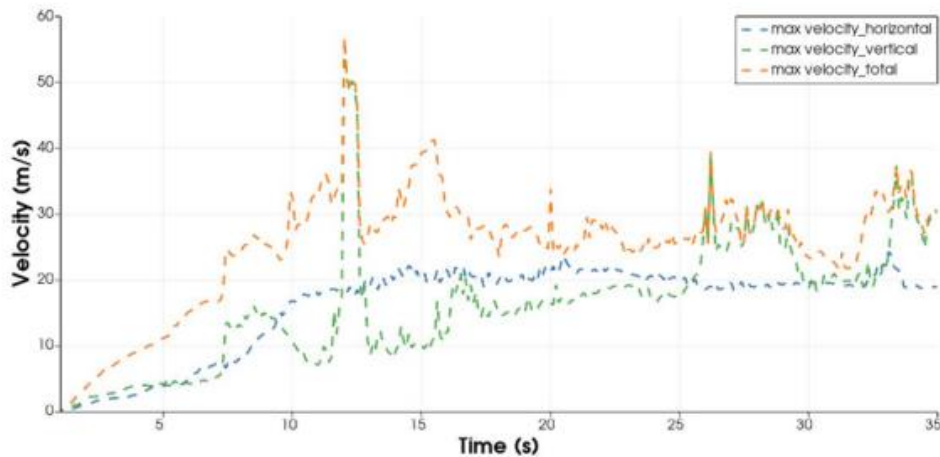
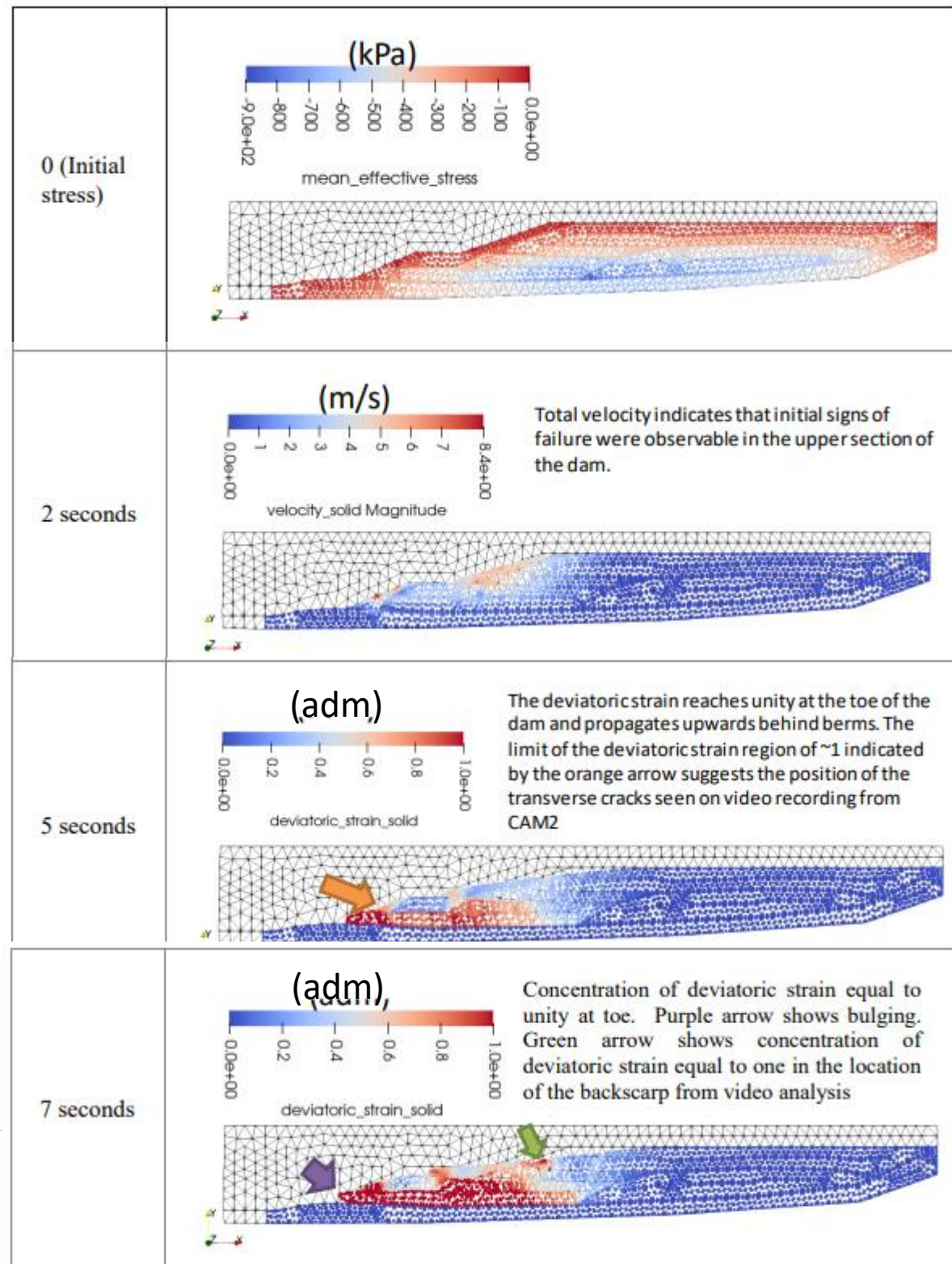


Figure 57: Change of Maximum Velocity during Failure as a Function of Time



Case studies

Cadia (Pierce 2021)

Using Anura3D

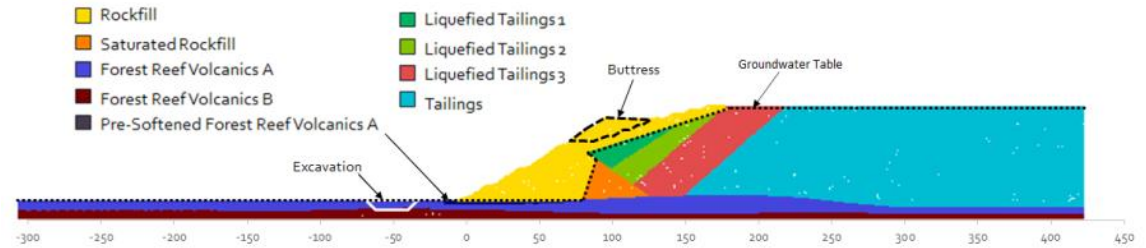


Figure 4.1: Reference Model Geometry (units in meters)

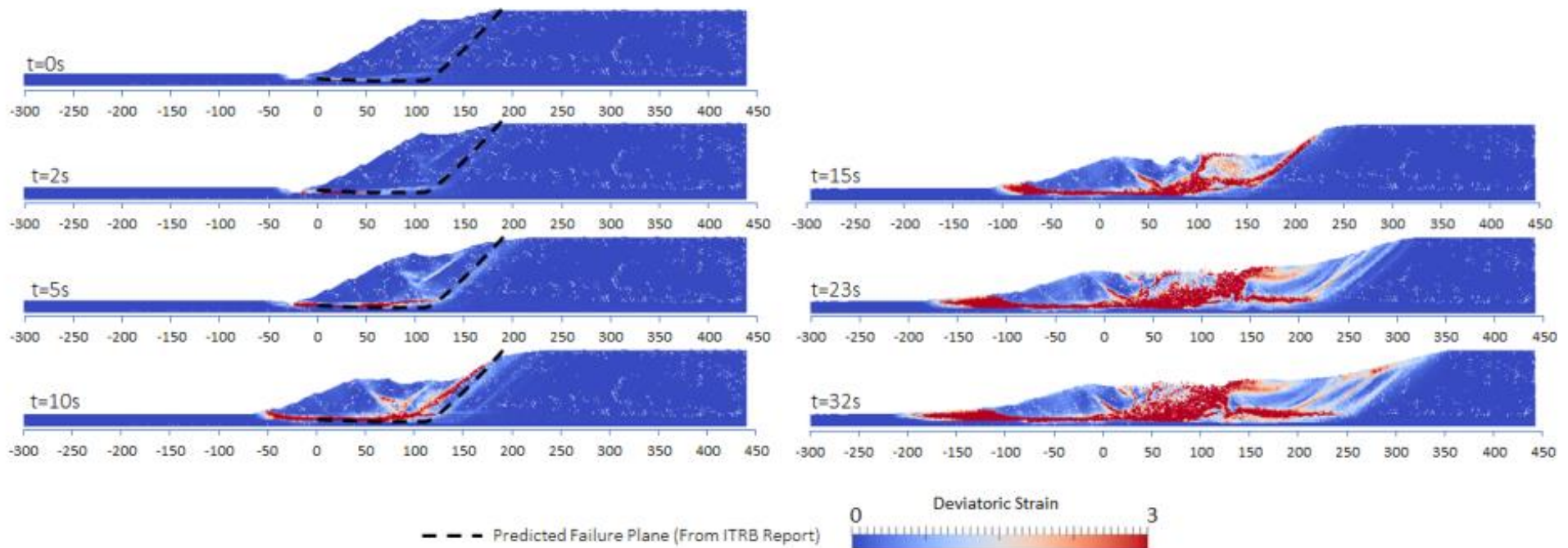


Figure 5.3: Failure plane progression through deviatoric strain at different times after the failure triggering (distance in meters)

Case studies

Cadia (Pierce 2021)

Using Anura3D

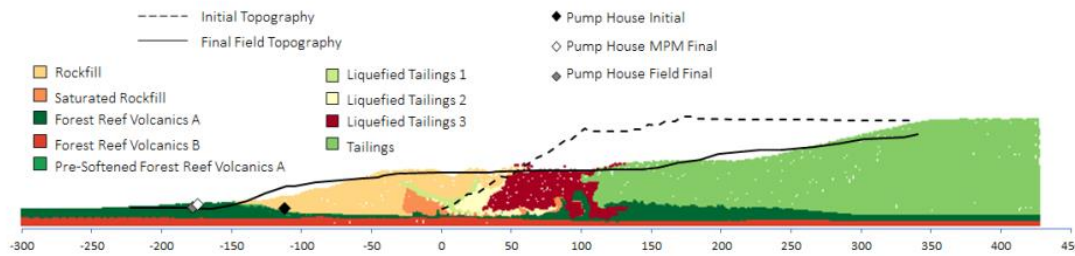


Figure 5.9: Final Runout: All Zones Liquefied at Failure Initiation (units in meters) [Model 6]

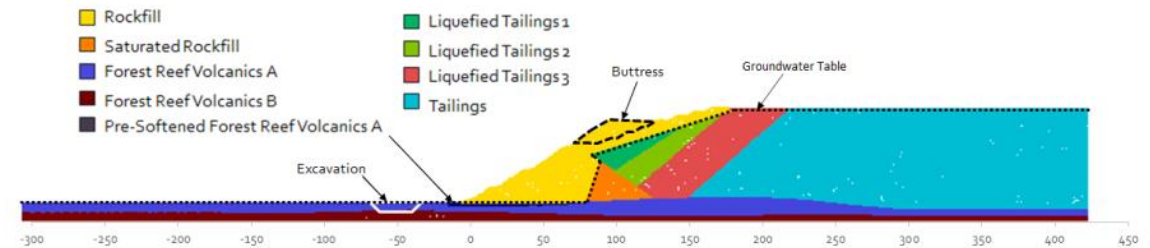


Figure 4.1: Reference Model Geometry (units in meters)

Key drivers of the observed behaviour were residual properties of the foundation, rate at which tailings liquified, the initial extent of liquified tailings, the presence of the excavation at the toe of the dam. The softening characteristics of the foundation played a large role allowing for the failure to occur, without the progressive softening of the foundation the dam does not move without the liquiefaction of tailings.

Summary and final thoughts

We have covered relevant aspects of the numerical modelling of tailings dam breaches from a soil's mechanics perspective. The review covered mobility of tailings, the role of large deformation modelling in TDBA, the relevance of the effective stress concept in tailings dam breaches and several case studies.

MPM is a growing technique. Although no commercial software is yet available, there is a vast technical resource on the web.

Despite all the advantages mentioned there are still limitations. Applicability is still limited to 2D problems, we offset this limitation by coupling the MPM outputs with hydraulic engineering software using the advantages offered by both techniques, which results in a better product for the clients. The publication of the recent GISTM with emphasis on ALARP concepts and the new CDA bulletin will likely accelerate the wider implementation of this (and other similar) type of approach in the industry.

Thanks,

marcelo@reearthengineering.com.au



Phase transformation and work required during dilation

The input energy per unit volume of soils was calculated to investigate its effect on the mechanical behaviour of sand samples prepared at loose and dense states using air pluvation.

The input energy per unit volume of specimens during an increment of straining in triaxial condition can be calculated as follows (Atkinson, 1993):

$$\delta W = q' \delta \varepsilon_s + p' \delta \varepsilon_v \quad (1)$$

in which, W is the energy (or work) done per unit volume of soil, q' is the deviatoric stress, ε_s is the shear strain, p' is the mean effective stress and ε_v is the volume strain (which is equal to zero in undrained triaxial tests). Table 2 shows the results of calculation of input energy in each phase of shearing response of the samples studied in this investigation.

Phase transformation occurs at axial strains of less than 5% and can consume a minimum of 95% of the energy required to shear the soil to axial strains of around 20%

Table 2. The input energy done on contraction and dilation phases of the tests.

Soil	Density condition	Confining pressure (kPa)	ε_{PT}^a (%)	W_{Con}^c/W_{Tot}^b (%)	W_{Dia}^d/W_{Tot} (%)
BP	Loose	100	2.32	1.53	98.47
BP	Loose	200	2.54	2.81	97.19
BP	Loose	400	3.21	3.62	96.38
BP	Loose	600	4.64	4.75	95.25
BP	Dense	100	0.74	0.29	99.71
BP	Dense	200	1.87	1.28	98.72
BP	Dense	400	1.92	1.62	98.38
BP	Dense	600	2.75	4.13	95.87
HI	Loose	100	1.19	0.59	99.41
HI	Loose	200	1.49	0.97	99.03
HI	Loose	400	2.61	1.68	98.32
HI	Loose	600	3.65	4.22	95.78
HI	Dense	100	0.37	0.11	99.89
HI	Dense	200	0.54	0.39	99.61
HI	Dense	400	1.13	0.84	99.16
HI	Dense	600	1.31	1.37	98.63

^a ε_{PT} : the axial strain at phase transportation phase

^b W_{Tot} : the entire input energy done at triaxial test

^c W_{Con} : the input energy done at contraction phase

^d W_{Dia} : the input energy done at dilation phase